

Model-agnostic Body Part Relevance Assessment for Pedestrian Detection

Maurice Günder^{1,2}[0000–0001–9308–8889], Sneha Banerjee^{1,3}[0000–0002–9950–2873],
Rafet Sifa^{1,2}[0009–0004–6680–8210], and Christian
Bauckhage^{1,2}[0000–0001–6615–2128]

¹ Fraunhofer Institute for Intelligent Analysis and Information Systems IAIS, Schloss
Birlinghoven, 53757 Sankt Augustin, Germany

maurice.guender@iais.fraunhofer.de

² University of Bonn, Institute for Computer Science III, Friedrich-Hirzebruch-Allee
5, 53115 Bonn, Germany

³ RWTH Aachen University, Department of Computer Science, Ahornstraße 55,
52074 Aachen, Germany

Abstract. Model-agnostic explanation methods for deep learning models are flexible regarding usability and availability. However, due to the fact that they can only manipulate input to see changes in output, they suffer from weak performance when used with complex model architectures. For models with large inputs as, for instance, in object detection, sampling-based methods like KernelSHAP are inefficient due to many computation-heavy forward passes through the model. In this work, we present a framework for using sampling-based explanation models in a computer vision context by body part relevance assessment for pedestrian detection. Furthermore, we introduce a novel sampling-based method similar to KernelSHAP that shows more robustness for lower sampling sizes and, thus, is more efficient for explainability analyses on large-scale datasets.

Keywords: Explainable AI · Model-agnostic explanations · Pedestrian detection · Autonomous Driving

1 Introduction

Today’s deep learning model architectures are more powerful than ever and enable the use of artificial intelligence (AI) in a wide range of application areas. However, with increasing model complexity comes increasing opacity and their output is less (human-)interpretable. Therefore, it is not uncommon for large models to be regarded only as black boxes. This can be particularly problematic in safety-relevant applications as, for instance, in autonomous driving (AD) where AI models cause decisions of autonomous systems that should be trustworthy, reasonable, and explainable. Thus, the field of Explainable Artificial Intelligence (XAI) is of increasing interest.

Generally, XAI approaches for analysis of deep learning models can be categorized in *model-specific* and *model-agnostic* methods. While model-specific methods are tailored to the underlying architecture and manipulate the test model in inference and/or training, model-agnostic methods are applied in a post-hoc manner to the test model, i.e., to fully trained models. These methods have the advantage of high flexibility, since models are treated as black boxes and, thus, any model can be analyzed the same way. Hence, the interpretation or explanation results can be compared across model classes or architectures. However, a major drawback of model-agnostic XAI methods is that only the model input can be manipulated to analyze consequential output changes. Therefore, these methods are sampling-based, which leads to a high computational effort for complex models.

In AD, the trustworthy recognition of street scenes, especially pedestrians, is of major interest. Contemporary object detection (OD) models show good performances, but have very different basic architectures and working principles. [7] For pedestrian detection, a severe challenge is that commonly, pedestrians appear under occlusion so that OD models have high robustness requirements here. [9] From an XAI point of view, it is therefore of particular importance on which semantic regions a test model bases its decisions for detecting a pedestrian and that those explanations can be compared regardless of the underlying test model architecture. Hence, model-agnostic explanation models should be considered here.

Model-agnostic explanation methods can be further distinguished into global and local explanation methods. Global methods try to explain the model on the data as a whole to interpret the overall performance, whereas local methods try to explain outputs for single data points or instances. Testing with Concept Activation Vector (TCAV) is a method that tests a model for relevant features that are given by example images [4]. A Concept Activation Vector (CAV) then quantifies the extent to which the model was activated in a prediction to a given concept. Those concepts can be, for instance, textures, color schemes, or anything that is describable by a bunch of images. Since we want to assess body parts, we don't have clear color or textures we want to focus on, and example images of isolated body parts are not available. This is why we do not focus on the TCAV in this work. Local Interpretable Model-agnostic Explanations (LIME) is a method for local explanation of instances by introducing a surrogate model that is simpler and more interpretable than the typically complex reference model [10]. The surrogate model, here, can be chosen arbitrarily which allows a lot of freedom in modeling but could end up in a surrogate model that is not human-interpretable. Shapley Additive Explanations (SHAP) tries to avoid this by defining a special LIME conform model that fulfills the properties of so-called Shapley values [11,6]. They originate from game theory and are well-defined and theoretically based measures for feature contribution to a certain outcome. The KernelSHAP method samples instances of present or absent features and, by observing the model output, it uses the so-called "Shapley kernel" to calculate the contribution of each feature to the output.

However, when it comes to OD problems, LIME and SHAP show some shortcomings being based on input sampling. In comparison to many machine learning tasks dealing with image processing, the input dimension and typically the model size is rather low, which makes single forward passes through the model quite fast. In image processing or, particularly, OD tasks, the input, i.e., image data, is rather complex and forward passes are computationally heavier. Thus, sampling images causes lots of forward passes decelerating the model explanation substantially. Due to the drastically larger number of input dimension, even more samples are needed to gain meaningful model explanations.

Therefore, we need to adapt sampling-based, model-agnostic explanation methods like KernelSHAP to explain the output pedestrian detection models.

2 Materials and Methods

We now shed light on how our approach to model-agnostic body part relevance assessment is structured. Figure 1 outlines the concept from the input street scene image to the so-called relevance maps. The details about the individual modules shown in this sketch are explained in the next sections.

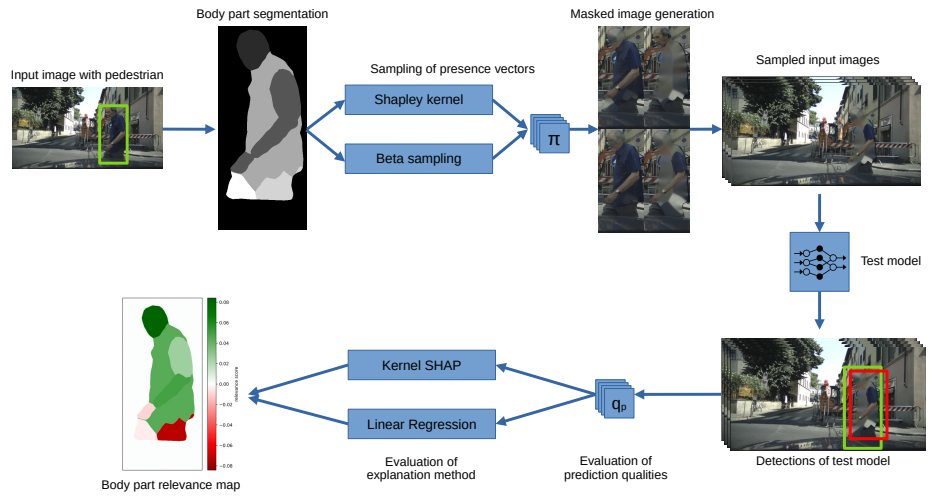


Fig. 1: Concept overview of our approach to model-agnostic body part relevance assessment.

2.1 Superpixel Model

In image processing like OD, the input size is typically much larger than for other machine learning tasks. Those large input sizes make sample based analyses

mostly infeasible due to the large combinatorial space. This is why the input size has to be drastically reduced in order to have efficient sampling. Moreover, the contribution of a single pixel to the actual detection can be considered to be negligibly small. Thus, a commonly used trick is to summarize a region of image pixels as a so-called *superpixel*. One way would be a fixed tiling into rectangular or quadratic superpixels, ignoring the actual image content. The other way is to define superpixels by semantic regions with similar texture, color, shape, or, in our case of pedestrian detection, body parts. In contrast to the fixed tiling, the semantic regions usually have different sizes.

The KernelSHAP method estimates the attribution of the input features to the output. Thus, we need to parametrize the superpixels by feature values. Our superpixel model, which serves as the explainable surrogate model, should have interpretable feature values. As we want to assess the relevance of body parts to the pedestrian detection, the feature values should represent the degree of information that is visible in the respective superpixel. Therefore, we introduce a *presence* value π_i for each superpixel i . A value of $\pi_i = 1$ means that the i -th superpixel is fully visible, as in the original input image. With decreasing presence value $\pi_i \rightarrow 0$, the superpixel gets increasingly hidden. In this work, we use three methods to hide the information of the superpixel. The first method is to overlay the superpixel with noise sampled from the information of the remaining image by a multinomial normal distribution given by the RGB information. The second method overlays the superpixel with noise sampled from the information of the neighboring superpixel contents. The third method is to remove all superpixels by a content-away *inpaint* method implemented in the OpenCV library [2]. A presence value of $\pi_i = 0$ means, that only the overlay is visible in the image, i.e., the superpixel information is completely hidden.

Thus, our superpixel model for the body part relevance assessment gets a presence vector $\boldsymbol{\pi} \in [0, 1]^k$ for k visible body parts as an input and samples an image based on this vector. This image is forwarded to the black-box OD model that should be analyzed. Figure 2 shows our three masking methods in the case of fully hidden body parts, i.e., $\boldsymbol{\pi} = \mathbf{0}$.

The typical output of an OD model are labels, bounding box (bbox) coordinates, and classification scores. The number of those elements is dependent from the number of detected objects in the input image. Thus, we need to formalize the detection quality of a distinct pedestrian of interest among multiple possible detections with multiple bboxes and scores. For pure classification, the classification score would be enough, but for OD, it is desirable for a detection quality score to include information about the precision of the bbox, as well. Therefore, we calculate the Sørensen-Dice Coefficient (DICE) between our ground truth bbox and all detection’s bboxes defined by

$$\text{DICE}(A, B) = \frac{2|A \cap B|}{|A| + |B|}, \quad (1)$$

where A and B are the two bboxes of interest. We identify the correct bbox by the maximum DICE with the ground truth bbox G . To include also the pure

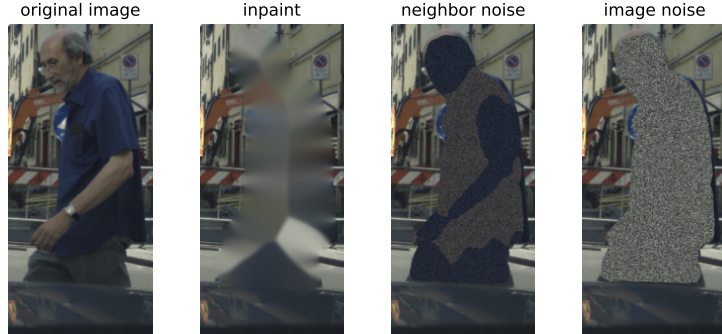


Fig. 2: Comparison of our masking methods demonstrated on a pedestrian image from the EuroCity Persons dataset [3].

classification quality, we multiply this value with the respective classification score c for the detection. Thus, our detection quality q_p of a pedestrian p with detected bounding box P is

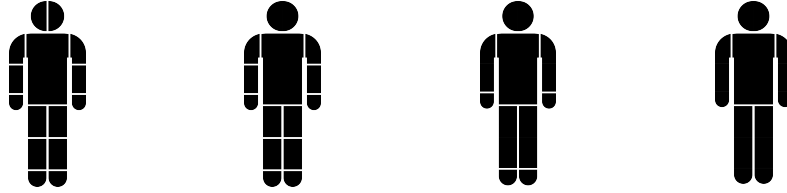
$$q_p = \text{DICE}(P, G) \cdot c_p. \quad (2)$$

Since DICE and c_p are values in the interval $[0, 1]$, it is $q_p \in [0, 1]$.

All in all, we now wrapped our OD model into a surrogate superpixel model, with an input vector and an output scalar.

2.2 Body Part Segmentation

In order to introduce the superpixel model parametrization to our pedestrian detection model, we need to get a segmentation of the body parts. For the currently available large-scale pedestrian datasets like CityPersons [12] or EuroCity Persons [3], proper body part segmentations are not available. Thus, we utilize *BodyPix*, a trained model for body segmentation [1]. BodyPix enables us to have vast amounts of real world pedestrian data. However, two major drawbacks are that the segmentation quality is rather low if the pedestrians resolution is low, i.e., for pedestrians appearing far away in the image. The other major drawback is that there is no instance segmentation available, which means that for pedestrian groups or multiple pedestrians in one bbox, we can only access the same body parts of all pedestrians at one time. At least, we can reduce the impact of the resolution problem by focusing our relevance assessment only on the biggest pedestrians, measured by bbox area, in the dataset of interest. By default, BodyPix segments 24 different body parts, including front and back parts. We can simplify our analysis by introducing 3 further mappings, where body parts are unified. We call those mappings *abstraction levels*, where level 0 is the original BodyPix output. The granularity reduces with ascending level number. The mappings are shown in Figure 3.



(a) Level 0. This is the original output of the BodyPix model. It has in total 24 body parts including front and back for the arm, leg, and torso parts. The orientations are w.r.t. the ego perspective.

(b) Level 1. In this first abstraction level, the two face halves are unified. Additionally, there is no differentiation of front and back parts. Overall, this results in 14 body parts.

(c) Level 2. In this second abstraction level, the upper and lower parts of arms and legs are unified, as well, resulting in 10 remaining body parts.

(d) Level 3. In this third abstraction level, hands are unified with the arms and feet are unified with the legs resulting in 6 remaining body parts.

Fig. 3: Abstraction levels of our body part segmentation. The levels represent the granularity from detailed (a) to less detailed (d).

2.3 From Sampling to Local Explanation

In KernelSHAP, one first defines an input and a baseline. The input is the instance to explain, so, in our case the visible pedestrian, i.e., we set $\pi_{\text{input}} = \mathbf{1}$ as the input. As the baseline, we set a completely absent or hidden pedestrian, thus $\pi_{\text{baseline}} = \mathbf{0}$. The sampling of the binary perturbation is weighted with the Shapley kernel and feature attribution values are calculated using weighted linear regression. [8] In this work, we will call those attribution values (*body part relevance scores*).

As mentioned, KernelSHAP perturbs the instance by masking features, so that all body parts can be absent or present and, hence, it does not consider our still possible partly presences with $0 < \pi_i < 1$. Therefore, we introduce a second custom sampling and explanation method using continuous sampling and, as well as KernelSHAP, linear regression to get the scores, but without following the Shapley properties. A uniform sampling of the presence values would end up in many “blended” body parts with is rather unrealistic. This is why we use a distribution that concentrates on values near 0 and 1. One distribution that has this property is the Beta distribution

$$B(x, \alpha, \beta) = \frac{\Gamma(\alpha + \beta)}{\Gamma(\alpha)\Gamma(\beta)} x^{\alpha-1} (1-x)^{\beta-1} \quad (3)$$

with the so-called concentration coefficients α and β . By deliberately choosing proper values for α and β , we can not only steer the concentration strength to the boundaries, but also the expectation value. In this work, for instance, we choose $\alpha = 0.2$ and $\beta = 0.1$ resulting in a distribution that is concentrated on

its limits at 0 and 1 with a slightly stronger concentration on 1. The expectation value results in an average pedestrian visibility of about 67%. An expectation value above 50% makes sense in our use case since otherwise, the pedestrian might often be not detected at all, resulting in a detection quality of 0. Thus, if too many generated samples end up in non-recognitions, we won't get insights in the relevance of body parts and the sampling becomes inefficient. Figure 4 shows a plot of the presence vector sampling probability density function (pdf) of our custom method. Another reason to concentrate the pdf on the limits is to have a robust linear regression even with a low amount of samples due to many data points at the outermost regions of the regression domain.

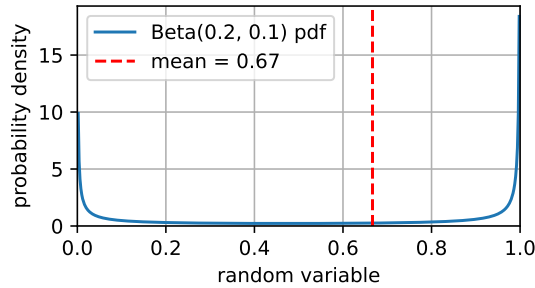


Fig. 4: Plot of the Beta distribution (Equation (3)), the presence vectors of our sampling method are drawn from. The red dashed line shows the expectation value (mean) of the distribution.

Once the presence vectors are sampled and propagated through the super-pixel and the OD model, we have the corresponding pedestrian detection quality scores and can calculate our body part relevance scores for both explanation methods by linear regression. The relevance scores can be visualized by the body part shapes with colors representing the respective relevance scores. We call those visualization *relevance maps*. Furthermore, we can estimate the error of the relevance scores of our method by performing 4 regressions with random 75% chosen from all data points. Means and standard deviations (stds) of those fits yield the relevance scores and errors, respectively.

3 Experiments and Results

In this section, we will perform a few experiments about comparability between KernelSHAP and our Beta sampling method. Additionally, since the number of samples is the crucial parameter that impacts the evaluation speed of both methods, we observe the stability of the relevance scores under small sample sizes. As a test model, we use a RetinaNet50 [5] object detection model trained on pedestrians from the EuroCity Persons [3] dataset.

3.1 Local Explanations

We evaluate KernelSHAP and our method by using our superpixel model for an example image from the EuroCity Persons dataset. For both methods, 2048 samples were drawn. In this case, the superpixel model uses the *inpaint* method to hide the body parts. The result is shown in Figure 5.

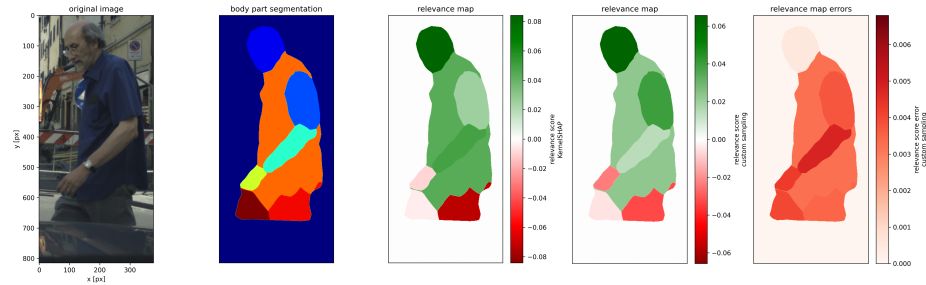


Fig. 5: Exemplary body part segmentation by BodyPix [1] and corresponding body part relevance maps of KernelSHAP (middle plot) and our sampling method (second from right). Additionally, an error map for our method is shown in the rightmost plot.

We notice, that the relevance scores calculated by KernelSHAP and our method are similar. Nevertheless, they show some minor differences. One problem in XAI is, that there is no “ground truth” explanation, especially not for model-agnostic methods. Thus, we treat the KernelSHAP results as the standard and try to compare our results with it because KernelSHAP has a heavier game theoretical basement due to the Shapley formalism.

3.2 Efficient Sampling

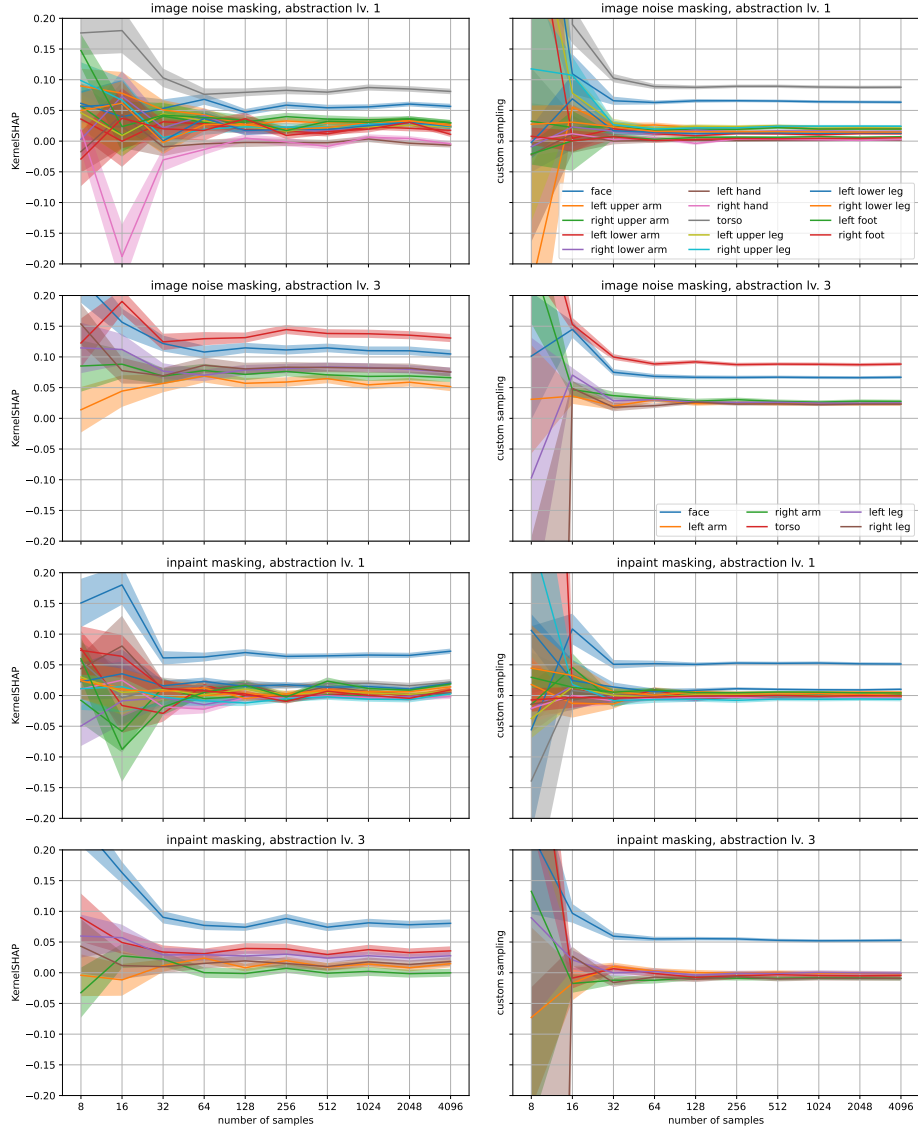


Fig. 6: Results of the sampling experiment for abstraction levels 1 and 3, image noise and inpaint masking, and KernelSHAP and our custom Beta sampling method. For each sampling size, the solid lines are the mean relevance scores for the biggest 100 pedestrians in the EuroCity Persons dataset. Transparent bands show the respective stds of the means.

In this experiment, we now want to see, how many samples we need at least, to get a fairly stable relevance score determination. We perform these experiments by using the first and third abstraction degree of body parts (see Figures 3b and 3d) and use inpaint and image noise masking. As sampling sizes, we use powers of 2 from 8 to 4096. In order to also cover, how the methods perform for different pedestrians, we perform the sampling on the 100 biggest pedestrians in the EuroCity Persons dataset regarding bbox size. Among those, 2 could not be segmented properly, so that 98 pedestrians contribute in the final results shown in Figure 6. In both abstraction degrees, body parts that do not undergo a merging with other body parts, namely face and torso, have agreeing relevance scores. A remarkable fact is, that the relevance scores differ among the masking methods. For instance, the torso has a significantly higher relevance score for the image noise masking than for the inpaint masking. However, comparing KernelSHAP with our Beta sampling method, we observe that Beta sampling yields more stable results. At 64 samples per pedestrian, the Beta sampling already gives results comparable to the higher sampling sizes. KernelSHAP, however, needs more samples to give converging relevance scores, if they converge at all. Conclusively, all experiment show, that our test model mainly focuses on torso and face regions which means that the clear presence or visibility of torso and head mainly drives the pedestrian detection quality.

4 Discussion

As already mentioned, KernelSHAP and our Beta sampling method yield comparable relevance scores. This makes sense by looking at the similar sampling properties. The Shapley kernel prefers samples with either very few or very many visible body parts, as shown in [8]. Even if the Beta sampling does not follow the Shapley properties exactly, the pdf is concentrated on 0 and 1 and, thus, samples are similar but with the difference of being non-binary. Therefore, we could say that the Beta sampling method is a continuation, or interpolation, of the Shapley kernel sampling.

The experiments show that our Beta sampling method requires fewer samples for robust relevance score assessment than KernelSHAP. Note that the two introduced methods in this work are local explanation methods per se. In order to gain insights into the global explainability of the test model, many local evaluations must be carried out, as we did in the experiments with many pedestrian instances. Thus, our method enables time-efficient analysis for large-scale datasets.

Nevertheless, a shortcoming in this work is the usage of the BodyPix body part segmentation model for the pedestrian detection. BodyPix is mainly used for high-resolution footage of human bodies. However, in street scene data, pedestrians are usually quite far away and, thus, have bad resolutions. Therefore, BodyPix can hardly segment proper body parts for those pedestrians. Additionally, BodyPix cannot discriminate different pedestrian instances, which is problematic in pedestrian detection since pedestrian occur in groups quite often

and bboxes overlap. This is why this work has to be seen as a proof-of-concept for the pedestrian detection use case. It is desirable to use our methods with datasets having available proper body parts and instance segmentation maps. To our knowledge, there is currently no such large-scale street scene dataset available.

5 Conclusion

Our work demonstrates, that KernelSHAP can be adapted to OD use cases. Moreover, the robustness can be increased by using non-binary sampling that is still similar to the Shapley kernel sampling. With specific reference to our application of pedestrian detection, it must be noted that BodyPix can only be used to a very limited extent for street scene shots due to the low resolution of the pedestrians. A possible starting point for further research would therefore be the use of simulation data, for which detailed semantic and instance segmentation maps are possibly rather available. Additionally, simulation data can further enrich the analysis by considering attributes beyond body parts like accessories or vehicles like bikes, wheelchairs, buggies, etc. Simulations also enable to gain data tailored to answer specific questions or scenarios that rarely appear in real-world data.

6 Abbreviations

AD autonomous driving
AI artificial intelligence
bbox bounding box
CAV Concept Activation Vector
DICE Sørensen-Dice Coefficient
LIME Local Interpretable Model-agnostic Explanations
OD object detection
pdf probability density function
SHAP Shapley Additive Explanations
std standard deviation
TCAV Testing with Concept Activation Vector
XAI Explainable Artificial Intelligence

References

1. Bodypix. <https://github.com/tensorflow/tfjs-models/tree/master/body-segmentation>
2. Bradski, G.: The OpenCV Library. Dr. Dobb's Journal of Software Tools (2000)
3. Braun, M., Krebs, S., Flohr, F.B., Gavrila, D.M.: Eurocity persons: A novel benchmark for person detection in traffic scenes. *IEEE Transactions on Pattern Analysis and Machine Intelligence* pp. 1–1 (2019). <https://doi.org/10.1109/TPAMI.2019.2897684>

4. Kim, B., Wattenberg, M., Gilmer, J., Cai, C., Wexler, J., Viegas, F., Sayres, R.: Interpretability beyond feature attribution: Quantitative testing with concept activation vectors (tcav) (2018)
5. Lin, T.Y., Goyal, P., Girshick, R., He, K., Dollár, P.: Focal loss for dense object detection (2017). <https://doi.org/10.48550/ARXIV.1708.02002>, <https://arxiv.org/abs/1708.02002>
6. Lipovetsky, S., Conklin, M.: Analysis of regression in game theory approach. *Applied Stochastic Models in Business and Industry* **17**(4), 319–330 (October 2001). <https://doi.org/10.1002/asmb.446>, <https://ideas.repec.org/a/wly/apsmbi/v17y2001i4p319-330.html>
7. Liu, L., Ouyang, W., Wang, X., Fieguth, P., Chen, J., Liu, X., Pietikäinen, M.: Deep learning for generic object detection: A survey. *International Journal of Computer Vision* **128**(2), 261–318 (Oct 2019). <https://doi.org/10.1007/s11263-019-01247-4>, <http://dx.doi.org/10.1007/s11263-019-01247-4>
8. Lundberg, S., Lee, S.I.: A unified approach to interpreting model predictions (2017)
9. Ning, C., Menglu, L., Hao, Y., Xueping, S., Yunhong, L.: Survey of pedestrian detection with occlusion. *Complex & Intelligent Systems* **7**(1), 577–587 (Oct 2020). <https://doi.org/10.1007/s40747-020-00206-8>, <http://dx.doi.org/10.1007/s40747-020-00206-8>
10. Ribeiro, M.T., Singh, S., Guestrin, C.: "why should i trust you?": Explaining the predictions of any classifier (2016)
11. Shapley, L.S.: A Value for N-Person Games. RAND Corporation, Santa Monica, CA (1952). <https://doi.org/10.7249/P0295>
12. Zhang, S., Benenson, R., Schiele, B.: Citypersons: A diverse dataset for pedestrian detection (2017). <https://doi.org/10.48550/ARXIV.1702.05693>, <https://arxiv.org/abs/1702.05693>